Draft version April 22, 2020
Typeset using LaTeX default style in AASTeX63

Neutron Star Masses and Equations of State

Emily Ramey[1] and Sergiy Vasylyev[1]

[1] *Department of Astronomy and Astrophysics, University of California, Berkeley, CA 94720, USA*

ABSTRACT

The study of Neutron Star (NS) masses has often been prone to uncertainty due to the very limited sample size of NS systems which have the required properties for mass measurement. However, the advent of gravitional wave astronomy and the detection of NS mergers by LIGO-Virgo Abbott et al. (2017) [only one data point here, although it presents a novel new way of measuring masses] has allowed more mass measurements to be made in recent years which have not been included in previous studies of the overall NS mass distribution. The goal of this paper is to review current research on the mass distribution of neutron stars and explore the important research problems facing the field today, such as the mass gap between NS and Black Holes (BH), constraints on the NS Equation of State (EoS), and possible limits on the maximum mass of a Neutron Star. *next couple sentences should be on our findings* We determine a gaussian Double Neutron Star mass distribution centered on $1.33 M_\odot$ with $\sigma = 0.17 \mathrm{M}_\odot$.

Keywords: neutron stars, mass limit, binaries

1. INTRODUCTION

The first binary pulsar, a system of radio-pulsing neutron stars, giving a reliable mass measurement was PSR B1913+16 [Hulse-Taylor 1975]. Since then, dozens of measurements have been made with improved precision using relativistic timing and spectroscopy techniques. A particularly surprising result is the observed gap between 3-5$M_\odot$ for compact objects. With the surge of Neutron Star (NS) mass measurements, this apparent region of missing mass has only become more significant, as shown in Figure **??**. As the number of observed neutron stars increased, key differences in the progenitors and environments became apparent. Thus, NS have been classified into 4 main groups: Double Neutron Stars (DNS), Recycled Pulsars (RPs), Bursters, and Slow Pulsars (SPs).

DNS systems consist of a pair of pulsars or NSs that lose their orbital energy to gravitational wave radiation. The NS-NS merger GW170817 detected by the Laser Interferometer Gravitational Wave Observatory (LIGO) and the Virgo interferometer in August 2017, falls into this category. RPs are old, primarily radio or x-ray emitting pulsars that have a white dwarf (WD) or main sequence (MS) companion. These pulsars are also referred to as "millisecond pulsars" describing their abnormally high spin caused by the accretion of gas from the companion. Through mass transfer from, these objects have been shown to spin up to as much as 716 Hz (CITE Hessels et al. 2006). Bursters or thermonuclear X-ray bursters are different from RPs in that their emission is primarily driven by thermonuclear processes, not through rotation or accretion. SPs are slow spinning objects that tend to be closely paired with a high mass companion.

Theoretical modeling of the NS Equation of State (EOS) is largely driven by observations, as our current understanding of matter in extreme gravity and density is limited. One of the probes for constraining the EOS is to obtaining the maximum mass of a NS, which is precisely the motivation for precise mass measurements. The EOS is commonly derived with respect to a fiducial density or a reference density (See Section 2.1). Precise limits on the maximum NS mass provide better constraints on this gap.

Here, we outline the current progress made in the search for a comprehensive Neutron Star equation of state (EOS) and highlight the recent measurements for a neutron star upper mass limit given the influx of new data and the rise of multi-messenger astronomy, including DNS merger GW170817. We compare the observationally inferred neutron star structure to the most up to date EOS models.

2. NEUTRON STAR EQUATION OF STATE

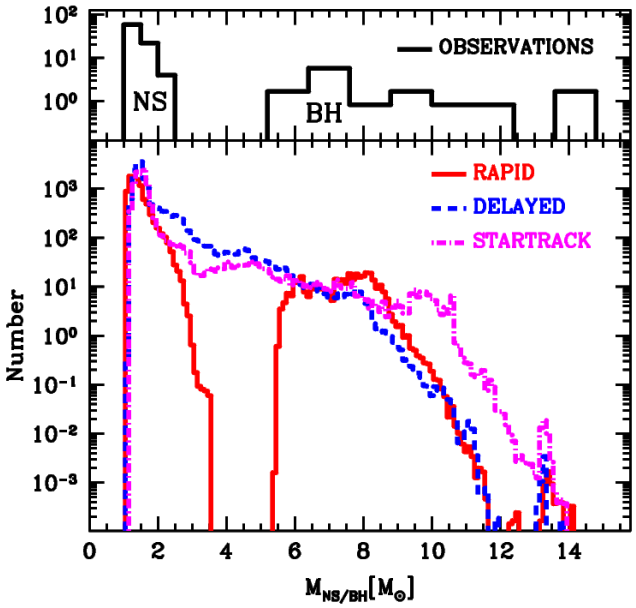

Figure 1. Top panel: Observational data of compact objects illustrating the mass gap from 3-5$M_{\odot}$. The red line and blue lines are the predicted mass distributions given a rapid and delayed supernova mechanism, respectively.[maybe insert timescale].The purple line shows the STARTRACK-modeled mass distribution, which favors a delayed supernova modelcite Belcyzinski et al. 2018

.

The Equation of State (EOS) of a neutron star is very difficult to calculate when taking the entire radius range. A naive approach assuming the NS consists primarily of non-relativistic, degenerate matter produces an upper limit of 5.8 $M_{\odot}$. In Section 4, we see that this model fails to explain the upper limit of around 2.2 $M_{\odot}$. Hence, we assume a special relativistic, degenerate state of matter to describe the equation of state.[Should we show the math here?] [Add a qualitative argument showing why relativistic correction allows for a more compressible NS, and therefore has a lower maximum mass than for the non-relativistic case]. In order to solve for EOS, we must also consider the effects of gravity, given the compactness of the NS.

2.1. *General Relativistic Hydrostatic Equilibrium*

We can get the pressure as a function of the neutron star's radius by integrating the Tolman-Oppenheimer-Volkoff (TOV) equation:

$$\frac{dP}{dr} = -\frac{G}{r^2}\left[\rho(r) + \frac{P(r)}{c^2}\right]\left[m(r) + 4\pi r^3\frac{P(r)}{c^2}\right]\left[1 - 2G\frac{m(r)}{rc^2}\right]^{-1} \tag{1}$$

The TOV is the General Relativistic form of the hydrostatic equilibium equation.

where the mass continuity equation applies:

Here, P(r) follows a polytropic form giving us our Equation of State (EOS):

$$P(r) = K\rho^{\Gamma} \tag{2}$$

In literature, the stiffness of the EOS to how steeply the pressure scales with density. The threshold for what is considered stiff is $\Gamma \geq 5/3$.[Might need citation].

MAXIMUM NEUTRON STAR MASS

Kalogera & Baym (1996) shows the theoretically derived mass limit in terms of the fiducial density ρ_0:

$$M_{max} = 6.7M_{\odot}\left(\frac{\rho_0}{10^{14}g * cm^3}\right)^{-1/2} \tag{3}$$

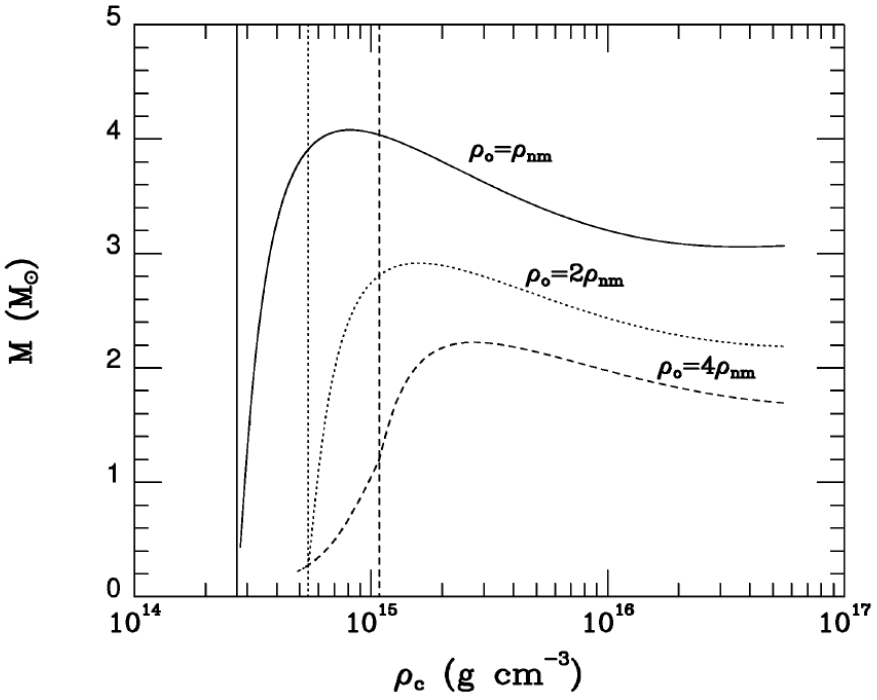

Figure 2. PLACEHOLDER FIGURE Kalogera & Baym (1996)

The observed M_{max} corresponds to a $\rho_0 \sim 3\rho_{nm}$, where $\rho_{nm} = 2.8 \times 10^{14}$g cm^{-3} the nuclear matter density.

3. MASS MEASUREMENT TECHNIQUES

Most known pulsar masses have been discovered through two primary techniques: relativistic pulsar timing combined with post-Keplerian physics and spectroscopy using Doppler shifts of strong lines. Only recently with the discovery of the DNS merger GW170817, have we been able to estimate the component masses in a binary neutron star system without relying solely on those two methods.

3.1. *Relativistic Pulsar Timing: Post-Keplerian Parameters*

From radio observations of pulsars, one can obtain 5 keplerian orbital parameters: the binary's orbital Period (P_b), the line-of-sight projected semi-major axis (x_{PSR}) measured in light-seconds, eccentricity (e), longitude (ω_0), and the time of periastron or closest approach to companion star (T_0). When gravitational effects are weak, the pulsar mass can be related to:

$$f = \frac{(M_c \sin i)^3}{M^2} = \left(\frac{2\pi}{P_b}\right)^2 x_{PSR}^3 T_\odot^{-1} \tag{4}$$

where M_c and M are the the companion mass and the total mass of the system, respectively. The pulsar mass is then $M_{PSR} = M - M_c$. Here, $T_\odot = GM_\odot/c^3$. In order to resolve the pulsar mass, one must obtain a constraint on the inclination i of the orbit and the companion mass. If the semi major axis of the companion can be measured and the companion is a white dwarf (WD) or main sequence star, then another parameter can be used to break the degeneracy in the equation above.

This extra parameter is defined as the mass ratio q:

$$q \equiv \frac{M_{PSR}}{M_c} = \frac{x_{PSR}}{x_c} \tag{5}$$

When gravitational dilation effects are taken into account, we must use the 5 post-Keplerian parameters defined in Section 3 b) of Taylor et al. (1992): 1) The rate of advance of the periastron $\dot{\omega}$, 2) the time delay due to gravitational-redshift effects known as the the Einstein delay γ, 3) the change in the orbital period $\dot{P}_b$, 4) the range of the Shapiro

delay r, and 5) the quantity related to the shape of the Shapiro delay s. The Shapiro delay is the delay in the time of arrival of information from a source due to light taking paths of different length through curved space-time around the source. This effect is amplified when viewing a binary system edge on or $i = 0$ deg. Possibly elaborate further on these parameters

It is a difficult task to measure these parameters. However, only two are needed to measure the pulsar mass M_{PSR} and the companion mass M_c. Examples of this pairwise requirement include J0348+0432 (q, M_{WD}), J0437-4715 (r, s), J0621+1002 ($\dot{\omega}$, s), J0751+1807 ($\dot{P}_b$, s) [CITE MWD Antoniadis et al. (2013), Reardon et al. (2016), Kasian (2012), Desvignes et al. (2016)]

3.2. *Doppler Spectroscopy*

Another way to measure the mass of a neutron star is through atomic spectral lines in the X-ray regime. For this method to be effective, the observed neutron star must have heavy metals in its atmosphere and a high enough temperature to emit significant thermal radiation. These features are characteristic of young pulsars, which have the required temperatures and frequently a high enough heavy metal fraction, and bursters, which renew their heavy metals through accretion and emit thermal radiation in large bursts due to shell burning. The atomic lines in the spectra of these neutron stars are subject to many relativistic effects, such as Doppler boosting, strong self-lensing, frame-dragging, and differential gravitational redshift. It is possible to infer the mass-radius ratio of a neutron star from the gravitational redshift, with a correction for the asymmetries caused by a nonspherical rotator. Relativistic Doppler boosting causes the spectral lines to be doubly peaked, with the peak separation depending on the neutron star radius. From these effects, both the mass and the radius can be inferred for a neutron star of known spin frequency. However, detecting atomic lines in the spectrum of a neutron star is very difficult due to heavy rotational broadening, and the asymmetries in the spectral lines introduce large systematic uncertainties into calculation. As a result, this method of measurement has too few candidates and remains too uncertain to effectively rule out most Equation of State models for pulsars (Ozel & Psaltis (2003)).

4. RESULTS

NEUTRON STAR MASS DISTRIBUTION

Although there have been on the order of 10^3 pulsars observed, only 10% are in binary systems (Abdo et al. 2013). Therefore, the current techniques relying on extracting mass information from orbital motion of the neutron star obtains a fairly small subset of the entire population. However, Precise Neutron Star (NS) mass measurements have been made using a variety of sources: Double Neutron Stars (DNS), Recycled Pulsars (RP), Bursters, and Slow Pulsars (SP). We add the newly discovered pulsars: J1811+2405 Ng et al. (2020), J2302+4442 Kirichenko et al. (2018), J2215+5135 Linares et al. (2018), J1913+1102 Ferdman & Collaboration (2017), J1411+2551 Martinez et al. (2017), J1757+1854 Cameron et al. (2018), J0030+0451 Riley et al. (2019), J1301+0833 Romani et al. (2016), since 2016 to the data from Ozel & Freire (2016), the mass distribution for which are shown in Figure 1. The recent GW170817 discovery provided another method of resolving the individual component masses in a NS binary. The upper mass limit for the primary NS is included in Figure 1 in red, where the error bars indicate a 90% confidence interval.

According to Figure 1, DNS observations provide the tightest bounds on the NS mass function with a standard deviation of $0.17 M_\odot$ compared to RPs with a standard deviation of $0.33 M_\odot$. Add mean value and sigma for RPs, no need to assume gaussian fit

Next, We employ an MCMC computation to determine the NS mass probability density function the using the bayesian model described in Kiziltan et al. (2010). [may add an Bayesian + MCMC computation treating each data point as a Gaussian to generate the mass distribution function (probability density function) similar to Kiziltan et al. (2010), more advanced version of figures 4 and 5]

CONSTRAINTS ON EOS

The inferred neutron star Equation of State (EOS) and therefore upper mass limit may vary for each of the different observational methods.

Should add color to the mass graph based on what measurement method was used, if we can find that info.

List observations from our compilation of NS Masses

We measured the mean NS mass at x, y, z with std dev of g, h, i for DNS, recycled pulsars, and slow pulsars,

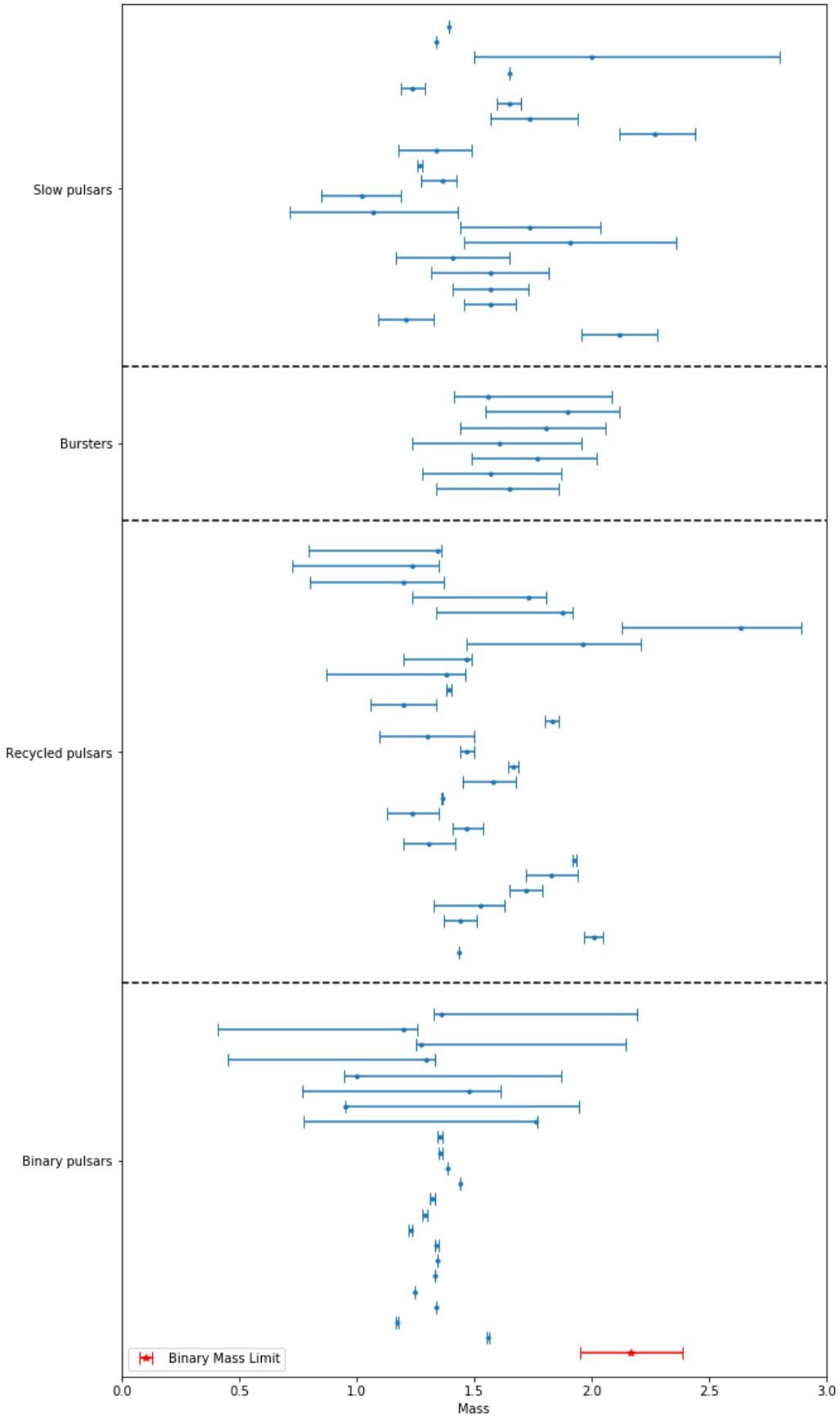

Figure 3. Inferred neutron star masses for source type using relativistic pulsar timing and Doppler spectroscopy. The upper mass limit obtained from the DNS GW170817 is shown in red. Margalit & Metzger (2017).

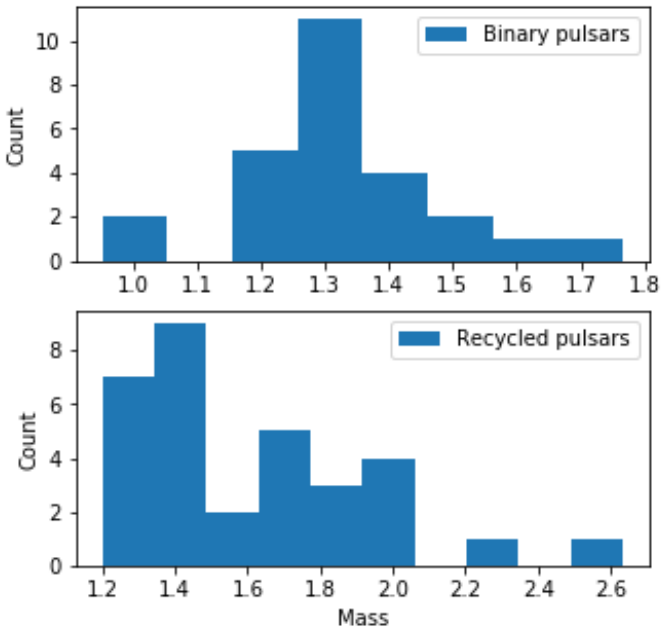

Figure 4. PLACEHOLDER Sample histogram of a mass distribution plot from Kiziltan et al. (2010)

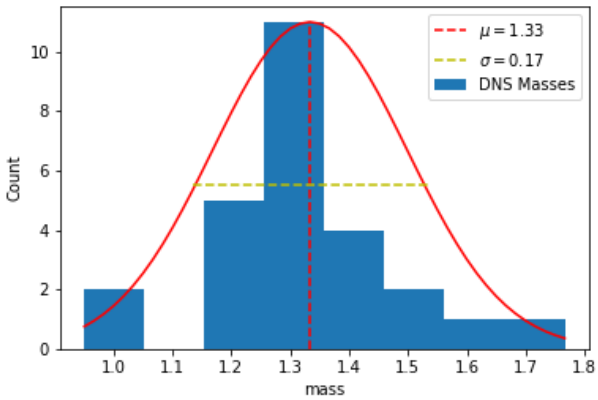

Figure 5. PLACEHOLDER Gaussian fit of DNS masses.

respectively. (Compare to literature values).
There is some evidence from tidal deformation studies that the mass gap between NS and BH is due to the difficulty of observing stellar remnants in that range.
Current measurements can also effectively rule out several EoS which?.

REFERENCES

Abbott, B., Abbott, R., Abbott, T., et al. 2017, Physical Review Letters, 119, 161101, doi: 10.1103/PhysRevLett.119.161101

Cameron, A. D., Champion, D. J., Kramer, M., et al. 2018, Monthly Notices of the Royal Astronomical Society: Letters, 475, L57, doi: 10.1093/mnrasl/sly003

Ferdman, R. D., & Collaboration, t. P. 2017, Proceedings of the International Astronomical Union, 13, 146, doi: 10.1017/S1743921317009139

Kalogera, V., & Baym, G. 1996, The Astrophysical Journal Letters, 470, L61, doi: 10.1086/310296

Kirichenko, A. Y., Zharikov, S. V., Zyuzin, D. A., et al. 2018, Monthly Notices of the Royal Astronomical Society, 480, 1950, doi: 10.1093/mnras/sty1978

Kiziltan, B., Kottas, A., & Thorsett, S. E. 2010, arXiv:1011.4291 [astro-ph, stat]. http://arxiv.org/abs/1011.4291

Linares, M., Shahbaz, T., & Casares, J. 2018, The Astrophysical Journal, 859, 54, doi: 10.3847/1538-4357/aabde6

Margalit, B., & Metzger, B. 2017, The Astrophysical Journal, 850, L19, doi: 10.3847/2041-8213/aa991c

Martinez, J. G., Stovall, K., Freire, P. C. C., et al. 2017, The Astrophysical Journal, 851, L29, doi: 10.3847/2041-8213/aa9d87

Ng, C., Guillemot, L., Freire, P. C. C., et al. 2020, Monthly Notices of the Royal Astronomical Society, 493, 1261, doi: 10.1093/mnras/staa337

Ozel, F., & Freire, P. 2016, doi: 10.1146/annurev-astro-081915-023322

Ozel, F., & Psaltis, D. 2003, The Astrophysical Journal, 582, L31–L34, doi: 10.1086/346197

Riley, T. E., Watts, A. L., Bogdanov, S., et al. 2019, The Astrophysical Journal, 887, L21, doi: 10.3847/2041-8213/ab481c

Romani, R. W., Graham, M. L., Filippenko, A. V., & Zheng, W. 2016, The Astrophysical Journal, 833, 138, doi: 10.3847/1538-4357/833/2/138

Taylor, J. H., Blandford, R. D., Hewish, A., Lyne, A. G., & Mestel, L. 1992, Philosophical Transactions of the Royal Society of London. Series A: Physical and Engineering Sciences, 341, 117, doi: 10.1098/rsta.1992.0088